THE IMPACT OF NUTRIENT LOADING ON NITROGEN REMOVAL AND CARBON DYNAMICS IN A *JUNCUS ROEMERIANUS* AND *SPARTINA ALTERNIFLORA* DOMINATED SALT MARSH IN THE NORTHERN GULF OF MEXICO

by

TAYLOR C. LEDFORD

BEHZAD MORTAZAVI, COMMITTEE CHAIR
JULIA A. CHERRY
OLIVA MASON

A THESIS

Submitted in partial fulfillment of the requirements
for the degree of Master of Science
in the Department of Biological Sciences
in the Graduate School of
The University of Alabama

TUSCALOOSA, ALABAMA

2019

ABSTRACT

Increased anthropogenic nutrient loading of nitrogen (N) and phosphorus (P) to estuaries and bays can lead to eutrophication, anoxia or hypoxia, and/or loss of native or other important species. Coastal salt marshes help to counteract eutrophication by removing excess N through microbially-mediated denitrification. One important factor that regulates salt marsh N removal is vegetation type, which affects sediment N-removal capacity by modifying redox potential and altering the microbial community structure within sediments. Additionally, plant community structure can alter carbon (C) uptake via photosynthesis and C release via sediment oxidation and organic matter degradation.

A 1-year field study was conducted in a salt marsh located on Dauphin Island, AL, where we increased N and P inputs by 20 g N m^{-2} yr^{-1}/ 1.25 g P m^{-2} yr^{-1} (low fertilization) and 40 g N m^{-2} yr^{-1}/2.5 g P m^{-2} yr^{-1} (high fertilization) in plots dominated by either *Juncus roemerianus* (black needlerush) or *Spartina alterniflora* (smooth cordgrass). Denitrification was 5X higher in unamended *J. roemerianus* plots versus *S. alterniflora,* but denitrification in *S. alterniflora* was more responsive to fertilization, increasing ten-fold while denitrification in *J. roemerianus* plots did not respond to fertilization. Gross primary productivity (GPP) was marginally higher (~5%) in control plots of *J. roemerianus* than in control *S. alterniflora* plots. High fertilization increased GPP by 27% in *S. alterniflora* plots, however, GPP did not respond to fertilization in *J. roemerianus* plots. Additionally, ER_{CO_2} was similar across vegetation types in control plots, and did not respond to fertilization in either vegetation type. Net ecosystem exchange was similar in *J. roemerianus* and *S. alterniflora* control plots and did not change in response to N and P

additions for either vegetation type. Our results illustrate that while both *J. roemerianus* and *S. alterniflora* marshes have the capacity to withstand nutrient loading in the Gulf of Mexico via N removal, *S. alterniflora* dominated marshes may have a greater capacity to mitigate N inputs. Additionally, in a world with higher nutrient inputs and despite higher GPP in *S. alterniflora*, both vegetation types will continue to sequester C at similar rates.

LIST OF ABBREVIATIONS AND SYMBOLS

±	plus or minus
%	percent
~	approximately
˚N	degrees north
˚E	degrees east
˚S	degreed south
˚W	degrees west
µM	micromolar
µmol	micromoles
µm	micrometer
ANAMMOX	anaerobic ammonium oxidation
˚C	degrees celsius
C	carbon
CO_2	carbon dioxide
CDOM	colored dissolved organic matter
cm	centimeter
d^{-1}	per day
DNRA	dissimilatory nitrate reduction to ammonium
DO	dissolved oxygen
ER_{CO_2}	ecosystem respiration

et al.	et alia (phrase meaning “and others”)
F	F-statistic (used when comparing statistical models to identify the model that best represents the original population from which the data where selected).
g	gram
GPP	gross primary productivity
GPS	global positioning system
hr^{-1}	per hour
HCl	hydrochloric acid
H_2S	hydrogen sulfide
I.D.	inner diameter
kg	kilogram
km	kilometer
KCL	potassium chloride
m	meter
m^2	square meter
m^{-2}	per square meter
mg	milligram
N	nitrogen
NH_4^+	ammonium
N_2	dinitrogen gas
NO_3^-	nitrate
NO_2^-	nitrite
NOx	nitrate plus nitrite
NEE	net ecosystem exchange

OM	organic matter
O_2	oxygen
P	phosphorus
PO_4^{3-}	phosphate
PSU	Practical Salinity Units (based on properties of water conductivity)
p	p-value (probability value which represents the smallest level of significance in which the null hypothesis is rejected)
rpm	rotations per minute
s^{-1}	per second
SE	standard error
UV	ultra-violet
χ^2	chi-square statistics (used to compare distributions of categorical data in two populations where the null hypothesis is rejected with smaller levels of significance (<0.05)).
yr^{-1}	per year

ACKNOWLEDGMENTS

Foremost, I would like to extend my sincerest appreciation to my advisor, Dr. Behzad Mortazavi of the University of Alabama for the continued help and valuable advice during the trials and tribulations of this document. This thesis would not have been possible without his support and guidance. Furthermore, I must also thank my other committee members, Dr. Julia A. Cherry and Dr. Olivia Mason, for their practical suggestions and helpful comments during this process.

I also wish to thank past and present members of the Mortazavi lab group: Dr. Corianne Tatariw, Alice Kleinhuizen, Patrick Chanton, Derek Tollette and Sommer Starr, for their continued moral support and assistance in the field and in the lab. Their wisdom and direction were extremely valuable and cannot be overestimated. Additionally, I would like to acknowledge Dr. Jeffrey Krause and Laura Linn from the Dauphin Island Sea Lab and Dr. Christina Staudhammer from the University of Alabama. Dr. Krause was generous enough to open up his lab and his spectrophotometer to me for numerous hours during this project, Laura's expertize and assistance in the analytical lab was critical, and Dr. Staudhammer greatly improved the quality of this work with her substantial knowledge of statistics, and for their help, I am grateful.

Finally, I would like extend my deepest thanks to my friends and my family, namely my mother, father, and sister whose continuous care and support never wavered during this experience.

CONTENTS

ABSTRACT ii

LIST OF ABBREVIATIONS AND SYMBOLS iv

ACKNOWLEDGMENTS vii

LIST OF TABLES x

LIST OF FIGURES xi

INTRODUCTION 1

METHODS 5

Study Site 5

Experimental Design 5

Site Characteristics 6

Porewater Analyses 7

Flux Measurements 8

Denitrification and ANAMMOX 9

DNRA 10

Statistical Analyses 11

RESULTS 13

Site characteristics 13

Sediment Characteristics 13

Porewater Analysis 14

CO_2 Flux Measurements 16

N-cycle Dynamics.....17
DISCUSSSION.....18
Species-specific Effects on Productivity 18
Species-specific Effects on N-removal.....20
Conclusions.....22
REFERENCES 32

LIST OF TABLES

1. Site Characteristics.....24

2. Sediment Characteristics.....25

3. Porewater Concentrations.....26

LIST OF FIGURES

1. Study Site Map.....27

2. Porewater Hydrogen Sulfide Concentrations.....28

3. CO_2 Flux measurements 29

4. N-cycle Dynamics.....30

5. Summary Figure.....31

INTRODUCTION

Human activity has more than doubled the amount of reactive N in the biosphere (Vitousek et al. 1997; Galloway et al. 2008). Watershed activities (i.e., industrial waste, sewage, agricultural runoff) associated with human population growth have been linked to high N inputs to rivers to coastal areas (Boesch 2002). As a result, N-limited coastal ecosystems such as estuaries, bays, and coasts (Howarth and Marino 2006) are more likely to become eutrophic globally (Nixon 1995; Rabalais et al. 2002; Smith 2003; Fabricius 2005). Due to the negative consequences of eutrophication, there is a need to understand the mechanisms of N cycling in coastal ecosystems, particularly processes that lead to permanent N loss.

Coastal marshes provide many ecosystem services such as nutrient filtering, flood control, erosion control and carbon (C) sequestration acting as a barrier between terrestrial upland and marine ecosystems (Valiela and Cole 2002; Fisher and Acreman 2004). Specifically, salt marshes reduce nutrient input to coastal systems by N-burial and microbially mediated denitrification, the step-wise reduction of nitrate (NO_3^-) to dinitrogen gas (N_2). Denitrification is of particular significance as it is a pathway of permanent N loss from the ecosystem (White and Howes 1994). This loss of N helps to mitigate the effects of eutrophication in coastal waters. However, incomplete denitrification can have consequential by-products, like nitrous oxide (N_2O), a harmful greenhouse gas. Furthermore, coastal marshes are among the most productive ecosystems in the world and act as natural C sinks reducing atmospheric carbon dioxide (CO_2) at a disproportionate rate to terrestrial systems (McLeod et al. 2011). Though they make up a small

percentage of the globe, net primary production can reach more than 600 g C m^{-2} yr^{-1} in coastal marshes (Chmura et al. 2003; Ouyang and Lee 2014). In addition to C sequestration via productivity, marshes can trap allocthonous C inputs making coastal marshes one of the largest natural C sinks, rivaling coral reefs and rain forests in C sequestration (McLeod et al. 2011).

Plant community assemblages inherently couple C and N cycling. Marsh vegetation alters sediment redox conditions which can influence substrate quality, and structure microbial communities (Mendelssohn and Postek 1982; McKee et al. 1988; Simpson et al. 2018). Vegetation is a significant source of sediment organic C, which acts as a universal electron donor for heterotrophic microbes (Beauchamp et al. 1989; Cherchi et al. 2009). Marsh vegetation also modifies sediment redox via root oxygen (O_2) translocation, promoting oxidized forms of N (NO_3^-), sulfur (SO_4^{2-}), iron (Fe(III)), as well as other electron acceptors. Increased oxygen availability in sediments promotes permanent removal of N via coupled nitrification/denitrification while simultaneously alleviating sulfur inhibition associated with the accumulation of toxic reduced sulfides (H_2S) (Bradley and Morris 1990; Rios-Del Toro and Cervantes 2016). In contrast, in marshes that are more reducing, or where sediment organic matter (OM) content is higher, recycling of N through dissimilatory nitrate reduction to ammonium (DNRA) is favored (Kraft et al. 2011; Hardison et al. 2015). DNRA is an additional NO_3^- reduction pathway in coastal marshes, which retains N in the form of NH_4^+ and has been found to make up 25% - 50% of nitrate reduction in salt marsh sediments (Giblin et al. 2013). Discerning the complex roles of marsh vegetation in N-removal versus N-retention and C sequestration is essential in understanding regional and global impacts of anthropogenic effluence and climate change.

Although vegetation type is a significant driver of linked C-N processes in salt marshes, few studies have linked C- and N- cycle processes as a result of chronic nutrient loading. In this study, we conducted a year-long fertilization of plots comprised of *Spartina alterniflora* and *Juncus roemerianus,* which are two common grasses found in salt marshes along the northern Gulf of Mexico. *Juncus roemerianus* is typically found in high marsh (Pennings et al. 2005) and has a more oxidized root/rhizome area (Gallagher and Plumley 1979), whereas *S. alterniflora* is typically found in the more reducing, low marsh area where concentrations of toxic H_2S can accumulate. However, our study site is unique in that *J. roemerianus* is interspersed throughout the *S. alterniflora* zone, resulting in minor elevation differences across experimental plots that permit examination of species-specific effects on C- and N-cycling. Seasonal rates of denitrification, anammox and DNRA, and monthly rates of CO_2 flux were measured to assess the effects of fertilization and vegetation type on C-storage and N-removal to further connect C- and N-cycles in coastal marshes.

Previous studies have found that *J. roemerianus* is typically more productive than *S. alterniflora* in salt marshes (Williams and Murdoch 1972; Hopkinson et al. 1980) due largely to the fact that above-ground biomass is typically close to double that of *S. alterniflora* (Gallagher 1975; Pennings et al. 2005; Joesting et al. 2016). Indeed, Starr et al. (2018) previously found that under ambient conditions, *J. roemerianus* productivity is higher than *S. alterniflora* at our study site. Similarly, *J. roemerianus* typically produces greater below-ground biomass than does *S. alterniflora* (Gallagher and Plumley 1979); thus, greater *J. roemerianus* root mass may have a greater rate of O_2 diffusion into surrounding sediments than *S. alterniflora*. Such differences would result in more reducing conditions in areas dominated by *S. alterniflora*. An additional factor controlling productivity is that coastal marshes are typically N-limited (Gallagher 1975;

Haines 1979; Mendelssohn 1979; Buresh et al. 1980; Cargill and Jefferies 1980; Cavalieri and Huang 1981; Delaune et al. 1986), so we expect that primary production would increase with N and P additions, regardless of vegetation type. Subsequently, greater plant productivity is expected to increase the amount of available C substrate to heterotrophic microbes; thus, heterotrophic processes like dissimilatory nitrate reduction (denitrification and DNRA) are expected to increase with fertilization. We hypothesized that after a 1-year fertilization treatment: 1) although biomass in both vegetation types was expected to increase, *J. roemerianus* plots would remain more productive than *S. alterniflora* plots post-fertilization; 2) N-removal via denitrification would be the dominant NO_3^- reducing pathway in *J. roemerianus* plots and would increase with fertilization; and 3) N-retention via DNRA would be the predominant pathway in the more reducing *S. alterniflora* plots and would increase with nutrient additions due to increased NO_3^- loading.

METHODS

Study Site

This study was conducted at a marsh located on the north side of Dauphin Island, AL, a subtropical barrier island 22.5 km in length and located in the northern central Gulf of Mexico at the terminus of Mobile Bay (30.2543° N, 88.1124° W, Figure 1). The south side of the island consists of beaches exposed to the Gulf of Mexico, while the north side consists of brackish ponds and back-barrier marshes. Dauphin Island receives ~ 2 kg N ha^{-1} yr^{-1} via atmospheric deposition (NADP 2016) and the average annual temperature range is ~13 - 28° C. Tides are diurnal with a mean tidal range of 0.36 m and tidal salinity averages of ~ 27 PSU. The dominant vegetation at the study site is *Spartina alterniflora* with patches of *Juncus roemerianus* interspersed throughout. Board walks were installed at each study plot prior to the initiation of the project to minimize damage to the marsh.

Experimental Design

Nine plots per species were chosen haphazardly at similar elevations (less than 3 cm difference across plots) for both *S. alterniflora* and *J. roemerianus* for a total of 18 plots. In addition to three ambient control plots, triplicate plots for low nutrient addition and high nutrient addition were included for each vegetation type. To provide a realistic assessment of nutrient loading rates in the southeastern USA, high and low treatments were based on loading rates

found in Mobile Bay, AL (~40 g N m^{-2} yr^{-1} & ~2.5 g P m^{-2} yr^{-1}) and Ochlockonee Bay, FL (~20 g N m^{-2} yr^{-1} & ~1.25 g P m^{-2} yr^{-1}), respectively (Twilley et al. 1999). N and P were added to each plot monthly via garden sprayers (Project Source 1.5 liter plastic tank sprayer) at low tide. Plots were separated by ≥ 1 m and enclosed in aluminum collars (0.26 m^2) to ensure adequate fertilization. Collars were embedded at 10 cm with holes at the sediment surface to allow natural drainage and inundation with the tidal cycle.

Site Characteristics

Elevation was taken at each experimental plot using a RTK GPS (Trimble-R8 Model-3 rover Trimble® Real Time Kinematic (RTK) GPS and TSC-2 controller). Point measures of water column salinity, dissolved oxygen (DO), and water temperature were taken seasonally at each site prior to each sampling period using a multiprobe (YSI model 556).

Above- and below-ground biomass was collected from *J. roemerianus* and *S. alterniflora* in areas outside of, but adjacent to, each experimental plot prior to fertilization to provide baseline comparisons. Additional above-ground and below-ground samples were taken from inside experimental plots at the end of the 1-year study to assess changes in vegetation morphology. Above-ground biomass within a 0.024 m^2 quadrat was cut at the sediment surface using clippers. The vegetation was brought back to the lab and dried at 70˚C to a constant weight. Below-ground biomass was collected using a metal T-corer (8.2 cm I.D.) inserted vertically to a depth of 15 cm. Cores were sectioned into 0-10 cm and 10-15 cm sections and wet sieved (2mm). The collected below-ground biomass was then dried at 70˚C to a constant weight.

Sediment syringe cores (1.3 cm I.D.) from each experimental plot were taken seasonally to a 1 cm depth and dried to a constant weight to obtain porosity and bulk density. Dried sediments were ground and homogenized with a mortar and pestle. Carbonates were then removed from the sediment via acid fumigation with 12N HCl for ~24 hours (Harris et al. 2001). Total sediment C and N was measured with a Costech Elemental Combustion System (Model 4010).

Separate sediment syringe cores (1.3 cm I.D.) from each experimental plot were collected to determine chlorophyll-a concentration to a 0-1 cm depth. The cores were returned to the lab and placed on a freeze-dryer for 48-72 hours. After freeze-drying, chlorophyll-a was extracted overnight at -20 ˚C with 90% acetone and analyzed with a Turner Designs TD-700 fluorometer set up for non-acidification method (Welschmeyer 1994).

Additional sediment cores (1.3 cm I.D.) were taken seasonally to 5 cm depth from each experimental plot for porewater extractable ammonium (NH_4^+). Homogenized sediment samples were extracted overnight on a shaker table with 2M KCl (Smith and Caffrey 2009). Following the extraction, the supernatant was filtered through glass fiber filters (GF/G 0.7 μm pore size) and frozen until analysis. Ammonium (NH_4^+) concentrations were determined with a Turner Designs 7200-002 fluorometer equipped with a CDOM/NH4 UV module (Holmes et al. 1999).

Porewater Analyses

Porewater sippers were installed permanently in each plot and allowed to equilibrate for at least 2 weeks prior to the beginning of the experiment. Sippers were equipped with a porous window at 10 cm depth (Porex, 24-40 μm pore size), which allowed for porewater collection as

described by Neubauer (2013). Sippers were purged of water and flushed with N_2 gas to remove oxygen prior to porewater collection. After 1 hour, duplicate porewater samples were extracted, GF/F filtered into 15 mL centrifuge tubes, and stored on ice until returned to the lab where they were frozen until analysis. Samples were analyzed colorimetrically for concentrations of NOx ($NO_3^- + NO_2^-$) and PO_4^{3-} using a UV-vis spectrophotometer as described by previous methods (Grasshof et al. 1983; Schnetger and Lehners 2014). NH_4^+ concentrations were analyzed as described above (Holmes et al. 1999). Additional porewater samples were taken for H_2S analysis and placed in N_2 flushed 12 mL vacuum-sealed Exetainers (Labco, Ceredigion,UK) with 50 µL of zinc acetate to preserve the sample. Samples were stored in the dark at room temperature until colorimetric analysis on a UV-vis spectrophotometer (Fonselius et al. 1983).

Flux Measurements

CO_2 fluxes were measured monthly with a transparent static chamber (0.26 m^2 x 1.02 m tall) placed on top of experimental plots as modified from Wilson et al. (2015). Holes in the side of the permanent collars were plugged with rubber stoppers and the edges of the collar were filled with water to allow an airtight seal. Within the chamber, three fans stirred the headspace and water was pumped through a heat exchanger to maintain an internal air temperature of ambient ± 2 ˚C. The chamber was allowed to equilibrate for 2 minutes before CO_2 measurements were taken with a gas analyzer (LI-COR. Lincoln, NE, USA model LI-820) in line with the chamber. Measurements at full light were taken every second continuously for 2 - 3 minutes to obtain net ecosystem exchange (NEE). The chamber was then lifted to equilibrate with the atmosphere, and then resealed and darkened. CO_2 was re-measured in the dark to obtain

ecosystem respiration (ER_{CO_2}). Gross primary productivity was then calculated from the difference in NEE and ER_{CO_2} (Equation 1), where NEE is the instantaneous flux into the marsh at full light and $ER_{CO_2}$is the flux into the marsh at zero light.

$$(1)\ GPP = NEE - ER_{CO_2}$$

Sampling was done during low tides on days with no rain and minimal cloud cover to allow for maximum light intensity and to limit water intrusion, which could inhibit gaseous diffusion from the soils.

Denitrification & ANAMMOX

Sediment cores (i.d. 2.6 cm) were collected from each experimental plot seasonally to a depth of 5 cm. Duplicate anoxic slurries were prepared using the sediment cores and artificial sea water (ASW) of a salinity consistent with the site water. Dinitrogen gas (N_2) was bubbled through the slurries to keep conditions anoxic. Slurries were siphoned into 12 mL Exetainers (Labco), leaving no headspace. The Exetainer slurries were placed on a shaker table (~70 rpm) in the dark overnight to equilibrate and to draw down residual NO_3^- and O_2. After removing from the shaker table, slurries were spiked to 50 µM (NO_3^-) with $Na^{15}NO_3^-$ (98 atom %, Cambridge Isotope Laboratories, Inc.) then recapped with no headspace. Samples received 200 µL of 50% w/v $ZnCl_2$ to stop microbial activity at 0 h (t_0) and 6 h (t_f) following $^{15}N\text{-}NO_3^-$ addition. The production of $^{29}N_2$ and $^{30}N_2$ was measured on a membrane inlet mass spectrometer (MIMS) to exclude any by-products from incomplete denitrification (Kana et al. 1994) using standard gas concentrations determined from Hamme and Emerson (2004). The mass spectrometer was

equipped with an inline copper column heated to 600˚C to remove residual O_2 from samples (Eyre et al. 2002).

Denitrification rates from sediment slurries were determined from the isotope pairing technique as described by Nielsen (1992):

$$(2)\ D_{15} = p29 + 2(p30),$$

where D_{15} represents denitrification of the added $^{15}N\text{-}NO_3^-$, and $p29$ and $p30$ represent the rates of $^{29}N_2$ and $^{30}N_2$ production, respectively.

$$(3)\ D_{14} = D_{15} + [\frac{p29}{2 \times p30}],$$

where D_{14} represents denitrification of the ambient $^{14}N\text{-}NO_3^-$

$$(4)\ D_t = D_{15} + D_{14},$$

where D_t represents the total denitrification or potential dentrification capacity.

Potential ANAMMOX rates in sediment slurries were determined from Thamdrup and Dalsgaard (2002):

$$(5)\ A_{total} = F_N^{-1} \times [P_{29} + 2 \times (1 - F_N^{-1}) \times P_{30}],$$

where A_{total} denotes production on N_2 through ANAMMOX, F_N is the fraction of ^{15}N in NO_3^-, and P_{29} and P_{30} represent the total produced mass of $^{29}N_2$ and $^{30}N_2$, respectively. ANAMMOX was less than 2% of the total nitrate reduction for both vegetation types, and therefore, will not be discussed in this study.

DNRA

Additional duplicate slurries samples were set up as described above to determine potential DNRA rates. Following the addition 200 µL of 50% w/v $ZnCl_2$, t_0 and t_f slurries were

bubbled with N_2 gas to remove any $^{29}N_2$ and $^{30}N_2$ resulting from denitrification and/or ANAMMOX. Then, the $^{15}NH_4^+$ product of DNRA was converted to $^{29}N_2$ and $^{30}N_2$ using an alkaline sodium hypobromite solution. Samples were analyzed on a MIMS for isotopic dinitrogen gas, and potential DNRA rates were determined using methods described by Yin et al. (2014):

$$(6)\ R_{DNRA} = \frac{[^{29+30}N_2]_{final} \times V - [^{29+30}N_2]_{initial} \times V}{W \times T},$$

where R_{DNRA} denotes the total, measured ^{15}N-based potential DNRA rates, $[^{29+30}N_2]_{initial}$ and $[^{29+30}N_2]_{final}$ represent concentrations of $^{15}NH_4^+$ in the initial and final samples of the slurry experiments, respectively, V is the volume (L) of the incubation vial, W denotes the dry weight (kg) of the sediment, and T is the duration of the incubation (h).

Statistical analyses

N-cycle dynamics (denitrification and DNRA), CO_2 flux measurements (GPP, NEE, and ER_{CO_2}), porewater chemistries (NO_x, PO_4^{3-}, and NH_4^+), and sediment characteristics (total C:N, chlorophyll-a, and porewater extractable ammonium) in control plots were tested with a 1-way ANOVA with vegetation type as a fixed factor in RStudio (v. 1.1.456; RStudio, Inc.) using NLME package (R core team; Pinheiro et al. 2018). To test responses to nutrient addition within each vegetation type, temporal and treatment-specific differences were assessed using a 2-way ANOVA on linear mixed effects models where fertilization treatment and month were included as fixed effects and plot location was treated as a random effect. A first-order autoregressive (AR(1)) covariance structure was estimated to characterize the correlation of time-dependent data, and the model with the lowest Akaike information criterion (AIC) value was used. Below-

ground biomass, above-ground biomass and sediment porosity were analyzed using a 1-way ANOVA with vegetation type as the factor in RStudio (Car package, R core team; Fox and Weisberg 2011). Plot-specific differences were determined using a Tukey's HSD or Kruskal-Wallis test when data were nonparametric. Normality and homoscedasticity were tested by visually inspecting plotted residuals. Equality of variances were tested using a Levene's test (Car package; R core team; Fox and Weisberg 2011).

RESULTS

Site characteristics

Elevation was statistically different for *J. roemericanus* and *S. alterniflora* plots with respect to NAVD88, though all plots were within 3 centimeters of each other (Table 1). Midday air temperatures at the study site ranged from 10.0˚C in March 2018 to 28.7˚C in July 2018. Soil temperatures ranged from 8.9˚C in January 2018 to 30.6˚C in June 2018. Porewater salinity ranged from ~12 PSU to ~29 PSU over the study period with no significant differences between species ($F_{(1,68)}$=3.393, p=0.0698). Prior to treatment, total aboveground biomass was 87% higher in patches of *J. roemerianus* than patches of *S. alterniflora* ($F_{(1,3)}$=47.8, p=0.002; Table 1), and belowground biomass was 63% higher in patches of *J. roemeranus* than *S. alterniflora* ($F_{(3,15)}$=27.2, p<0.05; Table 1).

Sediment Characteristics

Sediment C:N was slightly higher in *S. alterniflora* control plots than *J. roemerianus* control plots ($F_{(1,16)}$=5.8, p=0.03), but did not vary with fertilization treatment (*J. roemerianus*: $F_{(2, 18)}$=1.053, p=0.369; *S. alterniflora:* $F_{(2, 18)}$=0.219, p=0.8054) or season (*J. roemerianus*: $F_{(2,18)}$=2.280, p=0.131; *S. alterniflora:* $F_{(2,18)}$=2.944, p=0.0783) for either vegetation type. Similarly, sediment C content was higher in *S. alterniflora* plots than *J. roemerianus* plots prior to fertilization ($F_{(1,31)}$=5.5, p=0.03; Table 1), and did not vary with fertilization treatments (*J.*

roemerianus: $F_{(2, 18)}$=1.053, p<0.05; *S. alterniflora*: $F_{(2, 18)}$=0.219, p=0.05). Porosity was identical (0.77 ± 0.1; Table 1) prior to fertilization but was not measured after fertilizer additions. Sediment chlorophyll-a content was comparable across *J. roemerianus* and *S. alterniflora* control plots ($F_{(1,22)}$=0.7, p=0.41), and there was no treatment effect for either species (*J. roemerianus:* $F_{(2,23)}$=1.61, p=0.23; *S. alterniflora*: $F_{(2,24)}$=1.6, p=0.05). In *S. alterniflora* plots, sediment chlorophyll-a was highest in winter (~ 500 mg m^{-2}; $F_{(3,24)}$=11.009, p<0.05), but did not vary temporally in *J. roemerianus* plots ($F_{(3,23)}$=3.0, p=0.05).

Porewater extractable NH_4^+ concentrations were similar across *J. roemerianus* and *S. alterniflora* control plots ($F_{(1,22)}$=0.1, p=0.77) and did not differ across fertilization treatments for either vegetation type (*J. roemerianus:* $F_{(2,24)}$=0.7, p=0.51; *S. alterniflora:* $F_{(2,24)}$=1.4, p=0.26). Porewater extractable NH_4^+concentrations were lowest in summer, and comparable throughout the remainder of the year across both vegetation types (*J. roemerianus*: $F_{(3,24)}$=3.573, p<0.05; *S. alterniflora:* $F_{(3,24)}$=8.248, p<0.05).

Porewater Analyses

Total porewater NO_x concentrations were comparable in *J. roemerianus* and *S. alterniflora* control plots ($F_{(1,73)}$=1.2, p=0.27; Table 3) and did not differ across fertilization treatments (*J. roemerianus*: $F_{(2,66)}$=1.965, p=0.0148; *S. alterniflora*: $F_{(2,66)}$=0.083, p=0.920) for either vegetation type. Porewater NO_x concentrations did, however, vary temporally across both vegetation types, with no discernable pattern for either species (*J. roemerianus* peaked in March, June and November: $F_{(12,66)}$=4.837, p<0.05; *S. alternilfora* plots peaked in June and November: $F_{(12,76)}$=6.186, p<0.05).

Porewater NH_4^+ concentrations were similar in *J. roemerianus* and *S. alterniflora* control plots (Kruskal-Wallis; chi-squared=16.542, df=1, $p<0.05$; Table 3). NH_4^+ concentrations increased ~80% in fertilized *J. roemerianus* plots ($F_{(2,64)}= 7.0$, $p<0.05$), and ~40% in fertilized *S. alterniflora* plots ($F_{(2,70)}=8.8$, $p<0.05$). Porewater NH_4^+ concentrations varied temporally in *S. alterniflora* plots with highest concentrations in fall and winter (~200 µM; $F_{(12,70)}=44.7$, $p<0.05$), but there was no temporal effect on NH_4^+ concentrations in *J. roemerianus* plots ($F_{(12,64)}=7.7$, $p>0.05$).

Porewater PO_4^{3-} concentrations were comparable across *J. roemerianus* and *S. alterniflora* control plots ($F_{(1,74)}=0.2$, $p=0.07$; Table 3), and there was no effect of fertilization on PO_4^{3-} concentrations for either vegetation type ($F_{(2,71)}=2.6$, $p>0.05$ and $F_{(2,77)}=0.1$, $p=0.84$ for *J. roemerianus* and *S. alterniflora* plots, respectively). Porewater PO_4^{3-} concentrations varied temporally in *J. roemerianus* plots, with peak concentrations in fall and winter ($F_{(12,71)}=9.1$, $p<0.05$). There was no temporal variation in PO_4^{3-} concentrations in *S. alterniflora* plots, ($F_{(13,77)}=3.4$, $p>0.05$).

Porewater sulfides (H_2S) were 6x higher in *S. alterniflora* control plots than *J. roemerianus* control plots (1582.0 µM ± 191.4 SE and 261.0 µM ± 48.4 SE, respectively; $F_{(1,76)}=20.2$, $p<0.05$; Figure 2). Sulfide concentrations did not vary with fertilization treatment in either vegetation type ($F_{(2,71)}=2.9$, $p=0.63$ and $F_{(2,75)}=2.9$, $p>0.05$ for *J. roemerianus* and *S. alterniflora* plots, respectively), although concentrations seemed more variable in *S. alterniflora* plots. H_2S concentrations were highest in fall and winter in both vegetation types (October – December in *J. roemerianus* plots: $F_{(12,71)}=3.6$, $p<0.05$; October – January in *S. alterniflora* plots: $F_{(12,75)}=10.4$, $p<0.05$).

CO_2 flux measurements

Gross primary productivity was marginally higher in *J. roemerianus* control plots compared to *S. alterniflora* controls (20.6 µmol m^{-2} s^{-1} ± 2.1 SE and 19.6 µmol m^{-2} s^{-1} ± 1.4 SE, respectively; Kruskal-Wallis, p=0.05, χ^2=3.7, df=1; Figures 3e and 3f). There was no effect of fertilization treatment on GPP in *J. roemerianus* plots ($F_{10,66}$ =2.3, p=0.11). In contrast, high fertilization treatments increased GPP by ~27% in *S. alterniflora* plots ($F_{(10,64)}$ =12.12, p<0.02), though there was no effect of low fertilization treatment ($F_{(10,64)}$ =12.1, p=0.09). Highest GPP was measured in October in *J. roemerianus* plots (44.8 µmol m^{-2} s^{-1} ± 4.7 SE; Figures 4e and 4f), but otherwise did not vary throughout the study period ($F_{(10,66)}$ =8.1, p<0.05). There was no temporal effect on GPP in *S. alterniflora* plots ($F_{(10,64)}$ =1.3, p=0.24).

Ecosystem respiration did not differ between *J. roemerianus* and *S. alterniflora* control plots ($F_{(1,63)}$=0.6, p=0.44; Figures 3c and 3d). There was no effect of fertilization treatment on ER_{CO_2} in *J. roemerianus* plots ($F_{(10,66)}$=1.05, p= 0.36). As with GPP, high fertilization increased ER_{CO_2} by ~33% in *S. alterniflora* plots ($F_{(10,66)}$=6.30, p<0.05), although there was no effect of low fertilization treatment ($F_{(10,66)}$6.30, p=0.52). The highest ecosystem respiration was measured in September and October for both vegetation types (*J. roemerianus*: 11.8 µmol m^{-2} s^{-1} ± 0.9 SE, $F_{(10,66)}$ =3.648, p<0.05; *S. alterniflora*: 7.8 µmol m^{-2} s^{-1} ± 0.6 SE, $F_{(10,66)}$ =2.976, p<0.05).

Net ecosystem exchange was similar in *J. roemerianus* and *S. alterniflora* control plots (Kruskal-Wallis, p=0.24, χ^2=1.354, df=1, Figures 3a and 3b). There was no effect of fertilization treatment on NEE in either *J. roemerianus* plots or *S. alterniflora* plots (*J. roemerianus:* $F_{(10,66)}$ =1.85, p=0.17; *S. alterniflora:* $F_{(10,66)}$ =5.71, p=0.25). In *J. roemerianus* plots, highest NEE was measured in October (33.0 ± 7.5 µmol m^{-2} s^{-1}; Figures 4a and 4b), but was similar throughout the

remainder of the year ($F_{(10,66)}$=5.68, p<0.05). In contrast, there was no temporal effect on NEE in *S. alterniflora* plots ($F_{(10,66)}$=0.448, p=0.92).

N-cycle dynamics

Denitrification rates were ~5X higher in control plots of *J. roemerianus* than *S. alterniflora* (31.9 µmol N kg^{-1} hr^{-1} ± 6.8 SE and 6.4 µmol N kg^{-2} hr^{-1} ± 3.4 SE, respectively; $F_{(1,22)}$=12.8, p=0.002; Figures 4a and 4b). However, denitrification rates increased by ten-fold in fertilized *S. alterniflora* plots ($F_{(2,24)}$=16.8, p<0.05), while denitrification rates were similar across *J. roemerianus* fertilization treatments ($F_{(2,24)}$ =2.1, p=0.14). Denitrification rates varied temporally for both vegetation types, with lowest rates in summer (*J. roemerianus*: $F_{(2,24)}$=5.6, p=0.01; *S. alterniflora:* $F_{(2,24)}$=4.4, p<0.05).

DNRA rates were similar in *J. roemerianus* and *S. alterniflora* control plots (22.3 µmol N kg^{-1} hr^{-1} ± 3.7 SE and 29.6 µmol N kg^{-1} hr^{-1} ± 3.8 SE, respectively; $F_{(1,22)}$=1.9, p=0.18; Figures 4c and 4d). Unlike for GPP, ER_{CO2}, and denitrification, there was an effect of fertilization on DNRA in *J. roemerianus* plots, such that DNRA rates decreased ~55% in high fertilization plots ($F_{(2,23)}$=5.7, p<0.05). In contrast, DNRA rates did not vary with treatment in *S. alterniflora* plots ($F_{(2,24)}$=0.65, p=0.53). There was no significant temporal effect on DNRA rates for either vegetation type, although rates were slightly lower (~20%) in summer (*J. roemerianus*: $F_{(2,23)}$ =3.086, p>0.05; *S. alterniflora:* $F_{(2,24)}$ =3.626, p>0.05).

DISCUSSION

Species-specific effects on productivity

Our results demonstrate that vegetation type is a significant driver of primary productivity in marsh ecosystems. As hypothesized, GPP was higher in *J. roemerianus* control plots than *S. alterniflora* control plots; however, the difference was only marginal. *S. alterniflora*, a C4 species, is typically more efficient at photosynthesizing under salt stress, which can result in higher GPP per area biomass (Ehleringer and Monson 1993). Thus, differences in GPP between these species may be small despite *J. roemerianus* having significantly higher aboveground biomass per unit area.

Typically, inundation is described as an important driver of ER_{CO_2} (Burrows et al. 2005; Kathilankal et al. 2008; Jimenez et al. 2012; Starr et al. 2018), so it is expected in systems where clear elevational gradients are present, more inter-and intra-specific variation in ER_{CO_2} would occur. At our study site where *J. roemerianus* and *S. alterniflora* control plots are similar (within 3 cm difference), there are no differences in ER_{CO_2}, suggesting that, indeed, elevation is a more substantial driver of ER_{CO_2} than vegetation type. NEE was also similar between *J. roemerianus* and *S. alterniflora* control plots, which was attributed to the minor differences in GPP and ER_{CO_2} between species and the variability associated with GPP and ER_{CO_2}.

Increased loading of N and P into plots of *S. alterniflora* resulted in increased GPP and ER_{CO_2} (~27% and ~33%, respectively), whereas there was no effect of treatment among *J. roemerianus* GPP and ER_{CO_2}. These results indicate that, in a future of increased anthropogenic N and P inputs (Vitousek et al. 1997; Boesch 2002; Galloway et al. 2008), productivity responses will be largely facilitated by marsh vegetation type. Typically, coastal marshes tend to be N-limited (Sullivan and Daiber 1974; Patrick and Delaune 1976; Darby and Turner 2008). However, at our study site, *S. alterniflora* plants were likely P-limited, as indicated by high porewater ammonium concentrations prior to fertilization, yet productivity increased with further N and P additions. This phenomenon has been found by van Wijnen and Bakker (1999) in saltmarshes of the Netherlands where P-limitation occurs in the N-saturated environments, and also by Sundareshwar et al. (2003) in coastal marshes where P-limited microbes were affecting C-storage and C-release. There was no empirical evidence of N- or P- limitation in *J. roemerianus* plots during this study, which could suggest both N and P saturation.

Our results agree with previous results suggesting that ER_{CO_2} is closely linked to GPP, where a fixed portion of C is utilized for microbial respiration, and thus, an increase in GPP is often accompanied by an increase in ER_{CO_2} (Waring et al. 1998; Starr et al. 2018). Due to this productivity-respiration linkage, NEE does not vary across fertilization treatments in *S. alterniflora* plots, which can result in similar aboveground biomass pre- and post-fertilization.

Although our results do not show an effect of fertilization on NEE in plots of *J. roemerianus*, NEE tended to be highest at the end of the growing season in these plots, while NEE in *S. alterniflora* plots did not vary over time. These trends are also reflected in GPP, where *J. roemerianus* plots had the highest GPP at the end of the growing season while GPP in *S. alterniflora* plots did not vary over time. These results suggest that NEE is more directly driven

by GPP than ER_{CO_2}, whose temporal variation did not match NEE in either vegetation type. Also, shifts in source-sink regimes in coastal marshes seems to be mediated, in large part, by vegetation, where dominant vegetation type could be driving the overall net flux of CO_2 in or out of the marsh, which is important in the context of elevated atmospheric CO_2 levels associated with climate change.

Species-specific effects on N-removal

Typically, *Juncus* and *Spartina* species are separated by elevation (Pennings et al. 2005; Battaglia et al. 2012), creating vegetation zonation patterns driven by different redox potentials based on inundation stress (DeLaune et al. 1983; Mendelssohn and McKee 1988). Our results demonstrate that vegetation type is a critical controller of redox-driven biogeochemical processes such as denitrification, independent of large elevational gradients. We found that sulfide concentrations, a proxy for low redox potential (DeLaune et al. 1983; Devai and DeLaune 1995), were roughly seven-fold higher in *S. alterniflora* plots than *J. roemerianus* plotsm even when they occur at similar elevation (within 3 cm). We expect that this plant-driven difference in redox potential accounts for differences in denitrification potentials that were nearly 5X higher in *J. roemerianus* control plots. Joye and Hollibaugh (1995) found that soils with low redox potentials constrain N-removal via inhibition of coupled nitrification-denitrification, which is consistent with our results where denitrification was higher in *J. roemerianus* control plots. Although previous studies have shown that low redox potentials typically promote DNRA by providing hydrogen sulfide as a metabolic substrate (Tikhonova et al. 2006; Giblin et al. 2013), DNRA did not differ between the highly sulfidic *S. alterniflora* control plots and the less sulfidic *J.*

roemerianus control plots. This could result from the higher ambient concentrations of porewater NH_4^+ (the end product of DNRA) in *S. alterniflora* plots, thereby creating a negative feedback for the DNRA microbial community (McGlathery et al. 2007; Giblin et al. 2013).

Heterotrophic processes, like dissimilatory nitrate reduction (denitrification and DNRA), are often dependent on C substrate availability in subsurface sediments (Kraft et al. 2011; Hardison et al. 2015). Baas et al. (2014) found that increased photosynthetic production stimulates nitrification and N-fixation in coastal marshes resulting in concomitant increases in denitrification. This is reflected in the current study, where denitrification increased ten-fold in *S. alterniflora* plots with fertilization, accompanying increases seen in GPP and ER_{CO_2}. However, DNRA was similar across treatments in *S. alterniflora* plots, which further supports the idea that NH_4^+-saturation of the DNRA microbial community favored denitrification when NO_3^- was no longer limiting. Additionally, past studies suggest that higher C:N ratios typically favor DNRA over denitrification as the preferred NO_3^- reduction pathway; thus, the addition of NO_3^- would lower the organic C:N and ultimately favor denitrification (Tiedje 1982; Stremińska et al. 2012). Similarly, lower C:N ratios likely explain the decreased DNRA rates found in high nutrient addition *J. roemerianus* plots. The introduction of NO_3^- exceeds the introduction of new C, limiting DNRA and making denitrification the more favorable pathway in both vegetation types.

The greater denitrification response in *S. alterniflora* plots suggests that *S. alterniflora* has a greater capacity for removing excess nutrients in the short term. However, studies have shown that prolonged nutrient enrichment of salt marshes shifts plant productivity allocation from roots to shoots (Valiela et al. 1978; Schmidt et al. 2011), increasing marsh vulnerability to erosion and ultimate collapse (Deegan et al. 2012). In most marshes, *Spartina alterniflora*, in particular, may be more vulnerable due to its proximity to the marsh edge, which is more

susceptible to wave energy and flow, factors that are important to consider in the context of sea-level rise (Mariotti et al. 2010). However, single species vulnerability to marsh edge erosion is not always the case. Where marshes lack clear elevational gradients, similar to our study site, several species can be impacted by erosion and marsh collapse. Even though the results of our short term study showed increases in marsh function (N-removal and C-sequestration) in response to nutrient loading, it is important to consider long term impacts of nutrients and sea-level rise on marsh ecosystem structure.

The lowest denitrification and DNRA rates were found in July 2018 when soil temperatures were in excess of 30˚C in both *J. roemerianus* and *S. alternilfora* plots, suggesting that these heterotrophic processes could be temperature-dependent with an optimum temperature range below 30˚C. Previous studies report temperature optimums for denitrification between 25-30˚C with reduced activity above optimum (Saad and Conrad 1993; Kesik et al. 2006; Braker et al. 2010). By the years 2075 – 2099, global surface temperature is expected to rise 1-4˚C from the current temperature average with the areas in the northern Gulf of Mexico region rising as much as 2˚C (Biasutti et al. 2012). It is cause for further investigation if this increase in surface temperature could further affect the rates of biogeochemical processing and N-removal in coastal marshes, with consequences for eutrophication being linked to climate change.

Conclusions

The main goal of this study was to assess species-specific effects on N-removal and C-sequestration in response to increased nutrient loading to further understand the links between C- and N-cycles in salt marshes. Our results suggest that under current nutrient loading rates, *J.*

roemerianus marshes may have a greater capacity for N-removal and C-sequestration than *S. alterniflora* marshes. However, after a 1-year long fertilization study, there was little response in N- and C-cycles of *J. roemerianus* plots, whereas *S. alterniflora* plots increased in primary productivity and N-removal, with rates rivaling that of *J. roemerianus* plots. Our findings indicate that at a 2-3-fold increase in N and P loads, *S. alterniflora* marshes may have a greater capacity to remove N and sequester C, two critical ecosystem services. However, external factors, such as temperature and NH_4^+ accumulation, may have inhibitory effects on these ecosystem processes, highlighting the need to consider the impacts of nutrient loading in the context of climate-driven disturbances, such as warming and sea-level rise.

Table 1. Site Characteristics. Site Characteristics taken from Airport Marsh prior to fertilization. Below-ground biomass (BB) taken from 10 cores in each vegetation type and averaged over 15 cm depth. Above-ground biomass (AB) is the total weight per unit area collected from each vegetation type (n=3). Values represent averages ± 1 standard error. Different letters indicate statistical differences between vegetation types ($p < 0.05$).

	J. roemerianus	*S. alterniflora*
Belowground biomass (kg m^{-2})	4.64 ± 0.35**a**	2.84 ± 0.15**b**
Aboveground biomass (kg m^{-2})	12.09 ± 0.76**a**	6.46 ± 0.30**b**
Elevation (cm)	9.71 ± 0.52**a**	6.51 ± 0.27**b**
% total C	12.64 ± 0.37**a**	14.36 ± 0.62**b**
% total N	0.95 ± 0.03**a**	0.90 ± 0.04**a**
Pre-fertilization soil C:N (mol:mol)	15.7 ± 0.21**a**	18.70 ± 0.72**b**
Porosity	0.77 ± 0.01**a**	0.77 ± 0.01**a**

Table 2. Sedimetnt Characteristics. Sediment concentrations of chlorophyll-a, total iron, extracted ammonium (NH_4^+) and sediment C:N ratios collected seasonally concurrent with N-cycle dynamics (n=3). Vegetation C:N was collected from shoots of *J. roemerianus* and *S. alterniflora* from treatment plots beginning in April 2018. Values represent averages ± 1 standard error.

Vegetation type	2017 - 2018 season	Fertilization treatment	Sediment Chl-a (mg m^{-2})	Total Iron (umol g^{-1} dry weight)	[NH4+] nmol g^{-1} dry weight	Sediment C:N (mol:mol)	Vegetation C:N (mol:mol)
J. roemerianus	Fall	Ambient	203.47 ± 22.8	38.44 ± 19.4	68.46 ± 14.2	15.45 ± 0.3	-
		Low	395.38 ± 24.5	30.41 ± 11.9	73.57 ± 4.9	15.53 ± 0.6	-
		High	323.80 ± 51.6	28.17 ± 7.5	121.02 ± 13.4	15.12 ± 0.5	-
	Winter	Ambient	419.19 ± 25.0	26.52 ± 4.2	67.85 ± 13.8	15.55 ± 0.6	-
		Low	325.30 ± 197.2	25.00 ± 4.9	86.21 ± 13.7	18.03 ± 1.9	-
		High	231.89 ± 26.9	22.83 ± 7.7	50.32 ± 13.2	16.87 ± 1.6	-
	Spring	Ambient	258.39 ± 43.2	22.06 ± 6.9	79.46 ± 28.5	16.70 ± 1.2	54.75 ± 9.6
		Low	377.19 ± 15.2	8.75 ± 2.3	53.67 ± 10.6	18.09 ± 1.5	43.63 ± 7.1
		High	239.26 ± 42.7	27.36 ± 10.5	81.97 ± 15.7	16.97 ± 0.8	55.93 ± 5.6
	Summer	Ambient	208.02 ± 40.4	7.5 ± 2.9	48.42 ± 35.8	-	-
		Low	163.18 ± 15.8	13.34 ± 4.6	25.79 ± 4.6	-	-
		High	165.42 ± 7.9	16.81 ± 6.5	46.19 ± 4.3	-	-
S. alterniflora	Fall	Ambient	272.59 ± 122.4	20.19 ± 2.8	105.23 ± 21.5	19.82 ± 1.9	-
		Low	200.29 ± 46.0	10.91 ± 1.5	111.49 ± 30.8	19.06 ± 1.6	-
		High	182.53 ± 46.9	19.22 ± 5.8	111.90 ± 34.6	18.49 ± 2.2	-
	Winter	Ambient	606.53 ± 116.0	15.92 ± 2.8	68.31 ± 7.0	16.96 ± 0.6	-
		Low	550.18 ± 141.3	15.29 ± 5.5	105.00 ± 13.5	16.03 ± 0.3	-
		High	381.4 ± 71.2	17.7 ± 3.3	52.93 ± 3.5	16.45 ± 0.4	-
	Spring	Ambient	256.33 ± 56.5	11.46 ± 2.5	83.10 ± 17.7	17.85 ± 1.6	33.78 ± 1.0
		Low	236.32 ± 65.4	9.15 ± 2.4	92.72 ± 17.3	17.79 ± 1.1	30.91 ± 1.6
		High	199.89 ± 75.5	11.3 ± 2.7	50.84 ± 5.4	17.72 ± 0.8	31.91 ± 0.85
	Summer	Ambient	193.40 ± 77.2	1.86 ± 0.2	25.95 ± 10.2	-	-
		Low	177.58 ± 9.5	2.43 ± 0.5	36.81 ± 3.7	-	-
		High	161.42 ± 11.5	2.73 ± 0.8	50.61 ± 11.6	-	-

Table 3. Porewater Concentrations. Seasonal porewater concentrations of NOx (NO_3^- + NO_2^-), ammonium (NH_4^+), phosphate (PO_4^{3-}), and salinity collected over 2017-2018 study (n=3). Values represent averages ± 1 standard error.

Vegetation type	2017 - 2018 season	Fertilization treatment	NO_x (uM)	NH_4^+ (uM)	PO_4^{3-} (uM)	Salinity (psu)
J. roemerianus	Fall	Ambient	0.57 ± 0.19	111.7 ± 25.2	3.94 ± 1.49	26.8 ± 2.3
		Low	0.61 ± 0.18	142.7 ± 25.6	5.47 ± 1.40	26.8 ± 1.0
		High	0.87 ± 0.31	152.5 ± 27.8	5.13 ± 1.71	26.7 ± 1.3
	Winter	Ambient	0.79 ± 0.23	52.4 ± 11.5	1.37 ± 0.54	24.1 ± 1.2
		Low	2.44 ± 1.12	73.9 ± 15.1	4.23 ± 1.20	24.0 ± 1.3
		High	3.53 ± 1.70	86.7 ± 24.2	2.94 ± 1.11	24.0 ± 0.7
	Spring	Ambient	1.02 ± 0.39	30.3 ± 6.6	1.06 ± 0.33	24.1 ± 1.0
		Low	1.23 ± 0.35	100.0 ± 30.8	2.02 ± 0.50	25.3 ± 1.8
		High	0.92 ± 0.23	85.0 ± 24.9	0.59 ± 0.17	24.5 ± 1.3
	Summer	Ambient	0.41 ± 0.18	16.0 ± 11.0	4.71 ± 1.28	20.0 ± 3.4
		Low	0.84 ± 0.54	31.2 ± 15.2	5.10 ± 1.30	22.5 ± 2.8
		High	0.80 ± 0.37	21.9 ± 10.8	4.21 ± 1.72	19.7 ± 2.9
S. alterniflora	Fall	Ambient	1.47 ± 0.35	201.5 ± 24.4	2.78 ± 0.27	21.3 ± 1.4
		Low	1.75 ± 0.56	256.7 ± 79.9	2.47 ± 0.40	21.7 ± 0.8
		High	1.13 ± 0.26	281.7 ± 73.7	3.68 ± 0.48	22.7 ± 0.6
	Winter	Ambient	0.47 ± 0.13	161.5 ± 24.8	1.68 ± 0.37	22.2 ± 1.2
		Low	0.48 ± 0.19	115.9 ± 30.6	2.66 ± 0.80	23.3 ± 0.8
		High	0.40 ± 0.13	150.1 ± 42.8	1.69 ± 0.33	24.4 ± 0.5
	Spring	Ambient	0.61 ± 0.19	150.7 ± 55.9	1.34 ± 0.21	22.6 ± 0.8
		Low	0.67 ± 0.25	57.6 ± 22.0	1.15 ± 0.40	22.4 ± 0.9
		High	0.77 ± 0.18	24.4 ± 9.4	0.80 ± 0.18	22.9 ± 1.0
	Summer	Ambient	1.64 ± 0.47	69.6 ± 29.0	2.50 ± 0.61	20.8 ± 0.5
		Low	0.76 ± 0.25	70.5 ± 33.6	2.85 ± 1.10	20.0 ± 0.7
		High	1.41 ± 0.66	46.7 ± 17.3	3.72 ± 0.70	20.3 ± 1.0

Figure 1. Study Site Map. Location of study site on Dauphin Island, Alabama, USA.

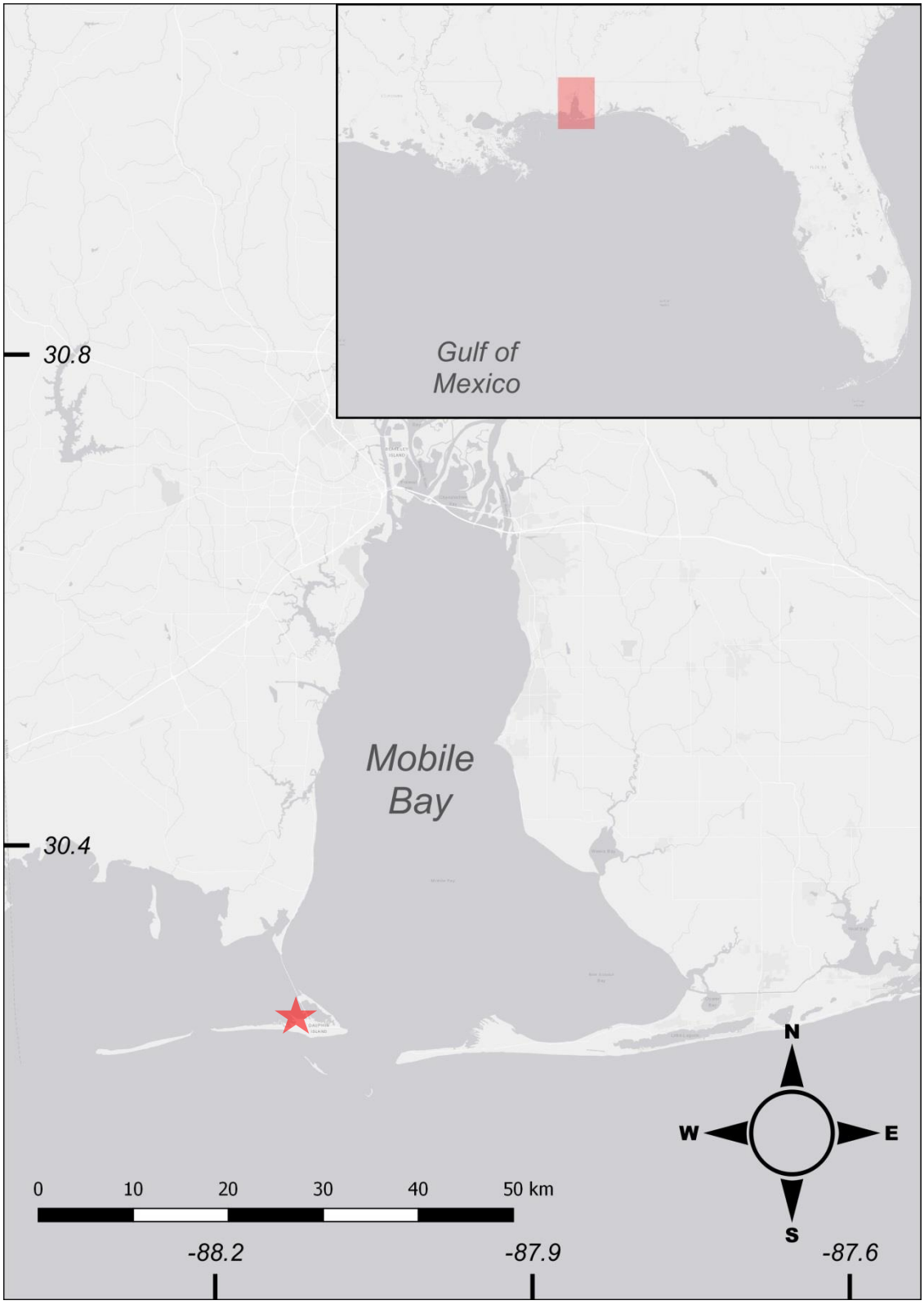

Figure 2. Porewater Hydrogen Sulfide Concentrations. Porewater H_2S concentrations (10 cm) from April 2017 to July 2018 in **a**) *J. roemerianus* and **b**) *S. alterniflora* patches (n=3). Error bars indicate averages ± 1 standard error.

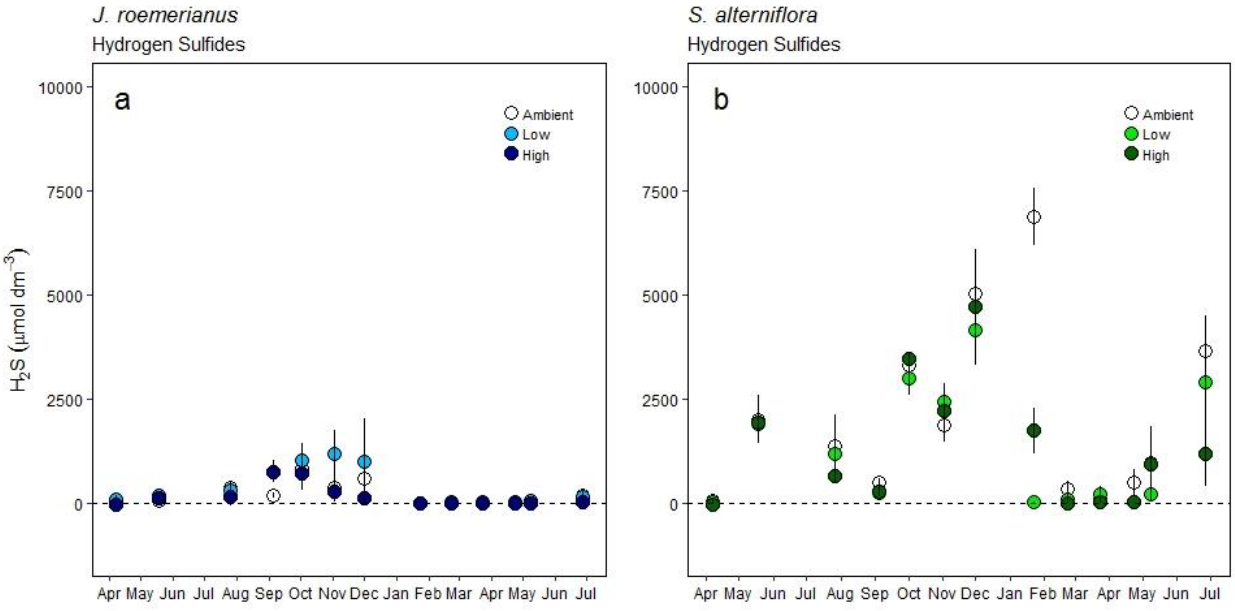

Figure 3. CO_2 Flux Measurements. CO_2 flux measurements for NEE, ER_{CO_2}, and calculated GPP in *J. roemerianus* (**a**, **c**, and **e**, respectively) and *S. alterniflora* patches (**b**, **d**, and **f**, respectively) (n=3). CO_2 Data was combined with environmental data taken from each sampling event. Error bars indicate averages ± 1 standard error.

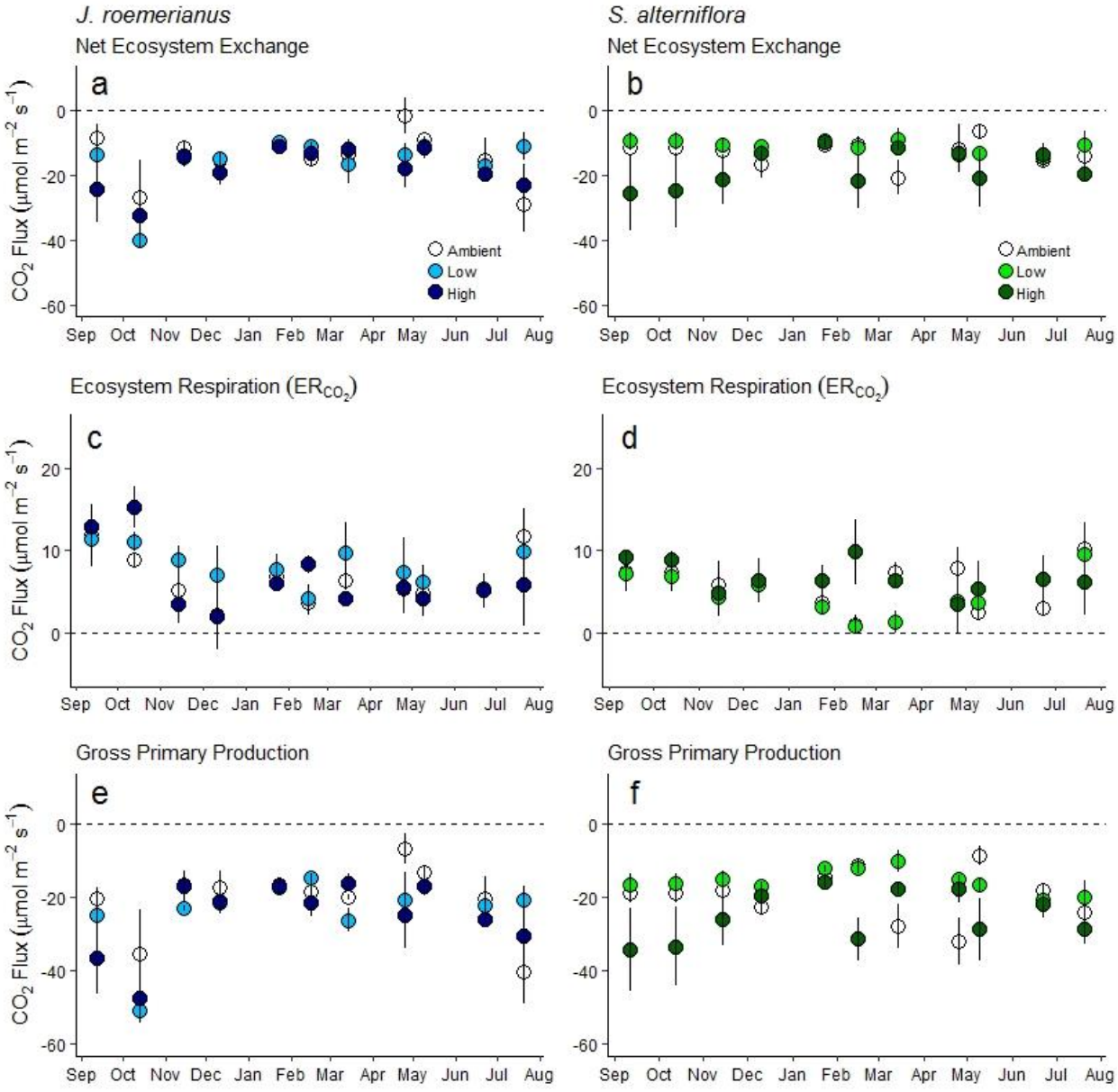

Figure 4. N-cycle Dynamics. Potential denitrification rates from **a**) *J. roemerianus* and **b**) *S. alterniflora* patches over the 2017-2018 study period (n=3). Potential DNRA rates from **c**) *J. roemerianus* and **d**) *S. alterniflora* patches over the study period (n=3). Error bars indicate averages ± 1 standard error.

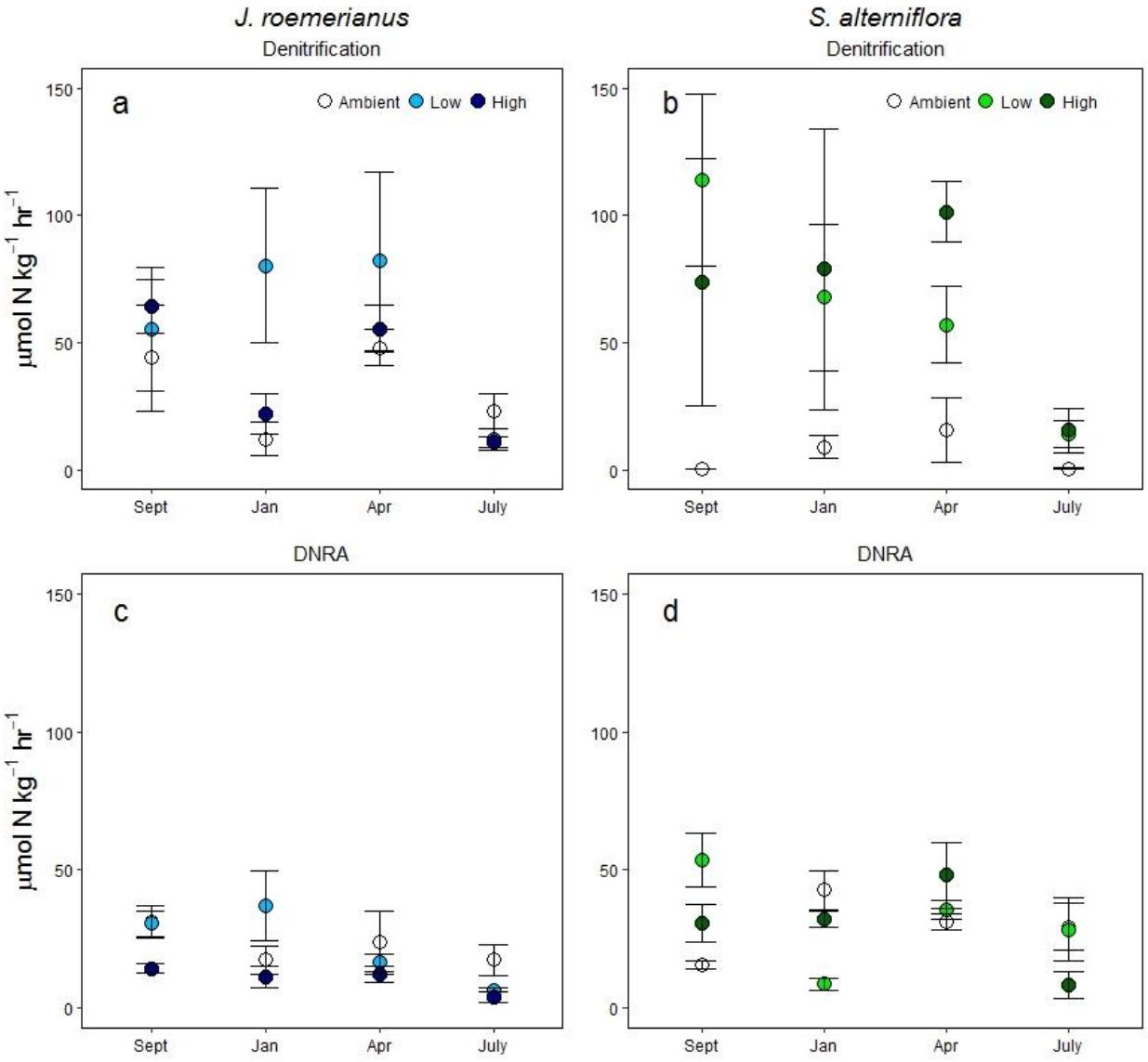

Figure 5. Summary Figure. Graphic summary representing averages of NEE, GPP, ER_{CO_2}, denitrification (DNF), and DNRA from control and fertilized *J. roemerianus* and *S. alterniflora* plots (n=3). Arrow direction indicates net gain (down) or net loss (up) from the marsh. Arrow sizes are relevant to the rates of losses or gains and asterisks indicate statistical significance ($p < 0.05$).

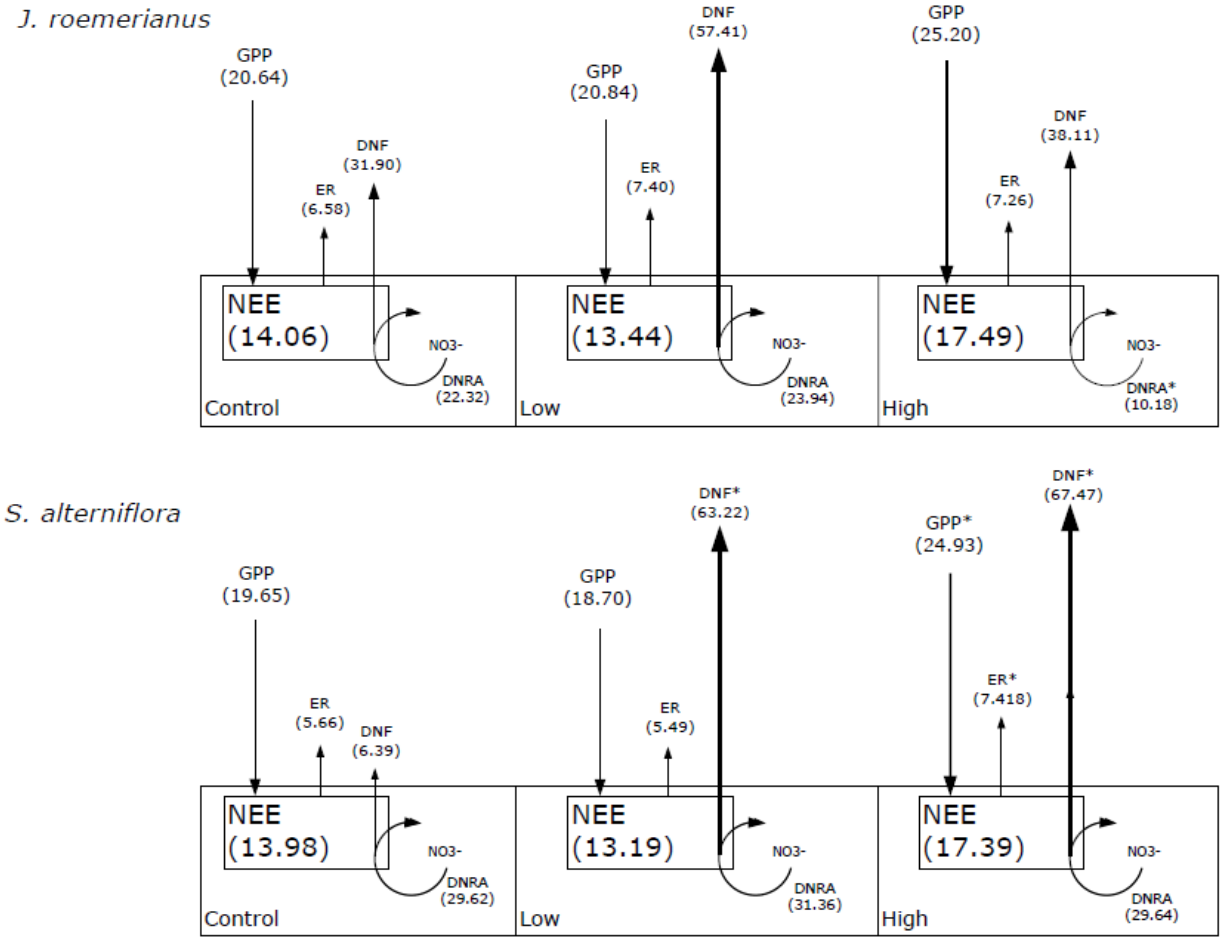

REFERENCES

Baas P, Hester MW, Joye SB (2014) Benthic primary production and nitrogen cycling in Spartina alterniflora marshes: Effect of restoration after acute dieback. Biogeochemistry 117:511–524. doi: 10.1007/s10533-013-9897-2

Battaglia LL, Woodrey MS, Peterson MS, et al (2012) Wetlands of the northern Gulf coast. In: Batzer DP, Baldwin AH (eds) Wetland habitats of North America: Ecology and Conservation Issues., illistrate. University of California Press, Berkely, pp 75–88

Beauchamp EG, Trevors JT, Paul JW (1989) Carbon sources for bacterial denitrification. 10:113–142. doi: 10.1007/978-1-4613-8847-0_3

Boesch DF (2002) Challenges and opportunities for science in reducing nutrient over-enrichment of coastal ecosystems. Estuaries 25:886–900. doi: 10.1007/BF02804914

Bradley PM, Morris JT (1990) Influence of oxygen and sulfide concentration on nitrogen uptake kinetics in *Spartina alterniflora*. Ecology 71:282–287

Braker G, Schwarz J, Conrad R (2010) Influence of temperature on the composition and activity of denitrifying soil communities. FEMS Microbiol Ecol 73:134–148. doi: 10.1111/j.1574-6941.2010.00884.x

Buresh RJ, Delaune RD, Patrick WH (1980) Nitrogen and phosphorus distribution and utilization by *Spartina alterniflora* in a Louisiana Gulf Coast marsh. Estuaries 3:111–121

Burrows EH, Bubier JL, Mosedale A, et al (2005) Net ecosystem exchange of carbon dioxide in a temperate poor fen: A comparison of automated and manual chamber techniques. Biogeochemistry 76:21–45. doi: 10.1007/s10533-004-6334-6

Cargill SM, Jefferies RL (1980) Nutrient limitation of primary production in sub-arctic salt marsh. J Appl Ecol 17:85–99. doi: 10.1097/01.mlg.0000167980.08493.30

Cavalieri AJ, Huang AHC (1981) Accumulation of proline and glycinebetaine in *Spartina alterniflora* Loisel . in Response to NaCl and Nitrogen in the Marsh. Ecology 49:224–228

Cherchi C, Onnis-Hayden A, El-Shawabkeh I, Gu AZ (2009) Implication of using different carbon sources for denitrification in wastewater treatments. Water Environ Res 81:788–799. doi: 10.2175/106143009X12465435982610

Chmura GL, Anisfeld SC, Cahoon DR, Lynch JC (2003) Global carbon sequestration in tidal, saline wetlands soils. Global Biogeochem Cycles 17:1164–1167. doi: 10.1029/2002GB001917

Darby FA, Turner RE (2008) Below- and aboveground *Spartina alterniflora* production in a Louisiana salt marsh. Estuaries and Coasts. doi: 10.1007/s12237-007-9014-7

Deegan LA, Johnson DS, Warren RS, et al (2012) Coastal eutrophication as a driver of salt marsh loss. Nature 490:388–392. doi: 10.1038/nature11533

DeLaune RD, Smith CJ, Patrick WH (1983) Relationship of marsh elevation, redox potential, and sulfide to *Spartina alterniflora* productivity. Soil Sci Soc Am J 47:930. doi: 10.2136/sssaj1983.03615995004700050018x

Delaune RD, Smith CJ, Sarafyan MN (1986) Nitrogen cycling in a freshwater marsh of *Panicum hemitomon* on the deltaic plain of the Mississippi River. J Ecol 74:249–256

Devai I, DeLaune RD (1995) Formation of volatile sulfur-compounds in salt-marsh sediment as influenced by soil redox condition. Org Geochem 23:283–287

Ehleringer JR, Monson RK (1993) Evolutionary and ecological aspects of photosynthetic pathway variation. Annu Rev Ecol Syst 24:411–439

Eyre BD, Rysgaard S, Dalsgaard T, Christensen PB (2002) Comparison of isotope pairing and N_2:Ar methods for measuring sediment denitrification-Assumption, modifications, and implications. Estuaries 25:1077–1087. doi: 10.1007/BF02692205

Fabricius KE (2005) Effects of terrestrial runoff on the ecology of corals and coral reefs: Review and synthesis. Mar Pollut Bull 50:125–146. doi: 10.1016/j.marpolbul.2004.11.028

Fisher J, Acreman MC (2004) Wetland nutrient removal : a review of the evidence. Hydrol Earth Syst Sci Discuss Eur Geosci Union 8:673–685

Fonselius S, Dyrssen D, Yhlen B (1983) Determination of hydrogen sulphide. In: Grasshof K (ed) Methods of Seawater Analysis, 3rd, Compl edn. Wiley-VCH, Weinheim, pp 91–100

Fox J, Weisberg S (2011) An R Companion to Applied Regression, 2nd edn. Sage, Thousand Oaks, CA

Gallagher JL (1975) Effect of an ammonium nitrate pulse on the growth and elemental composition of natural stands of *Spartina alterniflora* and *Juncus roemerianus*. Am J Bot 62:644–648

Gallagher JL, Plumley FG (1979) Underground biomass profiles and productivity in Atlantic coastal marshes. J Bot 66:156–161

Galloway JD, Townsend AR, Erisman JW, et al (2008) Transformation of the nitrogen cycle. Science (80-) 320:889–892. doi: 10.1126/science.1136674

Giblin A, Tobias C, Song B, et al (2013) The importance of dissimilatory nitrate reduction to ammonium (DNRA) in the nitrogen cycle of coastal ecosystems. Oceanography 26:124–131. doi: 10.5670/oceanog.2013.54

Grasshof K, Kremling K, Ehrhard M (1983) Methods of seawater analysis, 3rd, Compl edn. Wiley-VCH, Weinheim

Haines EB (1979) Growth dynamics of cordgrass, *Spartina alterniflora* Loisel., on control and sewage sludge fertilized plots in a Georgia salt marsh. Estuaries 2:50–53. doi: 10.2307/1352040

Hamme RC, Emerson SR (2004) The solubility of neon, nitrogen and argon in distilled water and seawater. Deep Res Part I Oceanogr Res Pap 51:1517–1528. doi: 10.1016/j.dsr.2004.06.009

Hardison AK, Algar CK, Giblin AE, Rich JJ (2015) Influence of organic carbon and nitrate loading on partitioning between dissimilatory nitrate reduction to ammonium (DNRA) and N_2 production. Geochim Cosmochim Acta 164:146–160. doi: 10.1016/j.gca.2015.04.049

Harris D, Horwath WR, Kessel C Van (2001) Acid fumigation of soils to remove carbonates prior to total organic carbon or carbon-13 isotopic analysis. Soil Sci Soc Am 65:1853–1856

Holmes RM, Aminot A, Kerouel R, et al (1999) A simple and precise method for measuring ammonium in marine and freshwater ecosystems. Can J Fish Aquat Sci 56:1801–1808

Hopkinson C, Gosselink JG, Parrondo RT (1980) Production of coastal Louisiana marsh plants calculated from phenometric techniques. Ecology 61:1091–1098

Howarth RW, Marino R (2006) Nitrogen as the limiting nutrient for eutrophication in coastal marine ecosystems: Evolving views over three decades. Limnol Oceanogr 51:364–376. doi: 10.4319/lo.2006.51.1_part_2.0364

Jimenez KL, Starr G, Staudhammer CL, et al (2012) Carbon dioxide exchange rates from short- and long-hydroperiod Everglades freshwater marsh. J Geophys Res G Biogeosciences 117:1–17. doi: 10.1029/2012JG002117

Joesting HM, Blaylock R, Biber P, Ray A (2016) The use of marine aquaculture solid waste for nursery production of the salt marsh plants *Spartina alterniflora* and *Juncus roemerianus*. Aquac Reports 3:108–114. doi: 10.1016/j.aqrep.2016.01.004

Joye SB, Hollibaugh JT (1995) Influence of sulfide inhibition of nitrification on nitrogen regeneration in sediments. Science (80-) 270:623–625

Kana TM, Darkangelo C, Hunt MD, et al (1994) Membrane inlet mass spectrometer for rapid high-precision determination of N_2, O_2, and Ar in environmental water samples. Anal Chem 66:4166–4170. doi: 10.1021/ac00095a009

Kathilankal JC, Mozdzer TJ, Fuentes JD, et al (2008) Tidal influences on carbon assimilation by a salt marsh. Environ Res Lett 3:. doi: 10.1088/1748-9326/3/4/044010

Kesik M, Blagodatsky S, Papen H, Butterbach-Bahl K (2006) Effect of pH, temperature and substrate on N_2O, NO and CO_2 production by *Alcaligenes faecalis* p. J Appl Microbiol 101:655–667. doi: 10.1111/j.1365-2672.2006.02927.x

Kraft B, Strous M, Tegetmeyer HE (2011) Microbial nitrate respiration - Genes, enzymes and environmental distribution. J Biotechnol 155:104–117. doi: 10.1016/j.jbiotec.2010.12.025

Mariotti G, Fagherazzi S, Wiberg PL, et al (2010) Influence of storm surges and sea level on shallow tidal basin erosive processes. J Geophys Res Ocean 115:1–17. doi: 10.1029/2009JC005892

McGlathery KJ, Sundbäck K, Anderson IC (2007) Eutrophication in shallow coastal bays and lagoons: The role of plants in the coastal filter. Mar Ecol Prog Ser 348:1–18. doi: 10.3354/meps07132

McKee KL, Mendelssohn IA, Hester MW (1988) Reexamination of pore water sulfide concentrations and redox potentials near the aerial roots of Rhizophora mangle and Avivennia germinans. Am J Bot 75:1352–1359

McLeod E, Chmura GL, Bouillon S, et al (2011) A blueprint for blue carbon: toward an improved understanding of the role of vegetated coastal habitats in sequestering CO_2. Front. Ecol. Environ.

Mendelssohn IA (1979) The influence of nitrogen level, form and application method on the growth response of *Spartina alterniflora* in North Carolina. Estuaries 2:106–112. doi: 10.2307/1351634

Mendelssohn IA, McKee KL (1988) *Spartina alterniflora* die-back in Louisiana : time-course investigation of soil waterlogging effects. J Ecol 76:509–521

Mendelssohn IA, Postek MT (1982) Elemental analysis of deposits on the roots of *Spartina alterniflora* Loisel. Ameri 69:904–912. doi: 10.2753/MTP1069-6679150101

Neubauer SC (2013) Ecosystem responses of a tidal freshwater marsh experiencing saltwater intrusion and altered hydrology. Estuaries and Coasts. doi: 10.1007/s12237-011-9455-x

Nielsen LP (1992) Denitrification in sediment determined from nitrogen isotope pairing technique. FEMS Microbiol Lett 86:357–362

Nixon SW (1995) Coastal marine eutrophication: A definition, social causes, and future concerns. Ophelia 41:199–219

Ouyang X, Lee SY (2014) Updated estimates of carbon accumulation rates in coastal marsh sediments. Biogeosciences 11:5057–5071. doi: 10.5194/bg-11-5057-2014

Patrick WH, Delaune RD (1976) Nitrogen and phosphorus utilization by *Spartina alterniflora* in a salt marsh in Barataria Bay, Louisiana. Estuar Coast Mar Sci 4:59–64. doi: 10.1016/0302-3524(76)90006-2

Pennings SC, Grant MB, Bertness MD (2005) Plant zonation in low-latitude salt marshes:

Disentangling the roles of flooding, salinity and competition. J Ecol 93:159–167. doi: 10.1111/j.1365-2745.2004.00959.x

Pinheiro J, Bates D, DebRoy S, et al (2018) Linear and nonlinear mixed effects models. R Packag version 31-137

Rabalais NN, Turner RE, Wiseman WJ (2002) Gulf of Mexico hypoxia, A.K.A. "The Dead Zone." Annu Rev Ecol Syst 33:235–263. doi: 10.1146/annurev.ecolsys.33.010802.150513

Rios-Del Toro EE, Cervantes FJ (2016) Coupling between anammox and autotrophic denitrification for simultaneous removal of ammonium and sulfide by enriched marine sediments. Biodegradation. doi: 10.1007/s10532-016-9759-4

Saad O, Conrad R (1993) Adaptation to temperature of nitric oxide-producing nitrate-reducing bacterial populations in soil. Syst Appl Microbiol 16:120–125

Schmidt MWI, Torn MS, Abiven S, et al (2011) Persistence of soil organic matter as an ecosystem property. Nature 478:49–56. doi: 10.1038/nature10386

Schnetger B, Lehners C (2014) Determination of nitrate plus nitrite in small volume marine water samples using vanadium(III) chloride as a reduction agent. Mar Chem 160:91–98. doi: 10.1016/j.marchem.2014.01.010

Simpson AG, Tripp L, Shull DH, Yang S (2018) Effects of *Zostera marina* rhizosphere and leaf detritus on the concentration and distribution of pore-water sulfide in marine sediments. Estuar Coast Shelf Sci 209:160–168. doi: 10.1016/j.ecss.2018.05.024

Smith KA, Caffrey JM (2009) The effects of human activities and extreme meteorological events on sediment nitrogen dynamics in an urban estuary, Escambia Bay, Florida, USA. Hydrobiologia 627:67–85. doi: 10.1007/s10750-009-9716-x

Smith VH (2003) Eutrophication of freshwater and coastal marine ecosystems: A global problem. Environ Sci Pollut Res 10:126–139. doi: 10.1065/espr2002.12.142

Starr G, Jarnigan JR, Staudhammer CL, Cherry JA (2018) Variation in ecosystem carbon dynamics of saltwater marshes in the northern Gulf of Mexico. Wetl Ecol Manag 26:581–596. doi: 10.1007/s11273-018-9593-z

Stremińska MA, Felgate H, Rowley G, et al (2012) Nitrous oxide production in soil isolates of nitrate-ammonifying bacteria. Environ Microbiol Rep 4:66–71. doi: 10.1111/j.1758-2229.2011.00302.x

Sullivan MJ, Daiber FC (1974) Response in production of cord grass, *Spartina alterniflora*, to inorganic nitrogen and phosphorus Fertilizer. Coast Estuar Res Fed 15:121–123

Sundareshwar, P.V., Morris, J.T., Koepfler, E.K & Fornwalt B. (2003) Phophorus limitation of coastal ecosystem processes. Science (80-) 5606:563–566. doi: 10.1126/science.1079100

Thamdrup B, Dalsgaard T (2002) Production of N_2 through anaerobic ammonium oxidation coupled to nitrate reduction in marine sediments. Appl Environ Microbiol 68:1312–1318.

doi: 10.1128/AEM.68.3.1312

Tiedje JM (1982) Denitrification. In: Page AL (ed) Methods of soil analysis. Part 2. Chemical and Microbiological properties, 2nd edn. Agron. Monogr., Madison, WI, pp 1011–1026

Twilley RR, Cowan J, Miller-Way T, et al (1999) Benthic nutrient fluxes in selected estuaries in the Gulf of Mexico. In: Bianchi TS, Pennock JR, Twilley RR (eds) Biogeochemistry of Gulf of Mexico Estuaries. Wiley-Liss, New York, pp 163–209

Valiela I, Cole ML (2002) Comparative evidence that salt marshes and mangroves may protect seagrass meadows from land-derived nitrogen loads. Ecosystems 5:92–102. doi: 10.1007/s10021-001-0058-4

Valiela I, Teal JM, Volkmann S, et al (1978) Nutrient and particulate fluxes in a salt marsh ecosystem: Tidal exchanges and inputs by precipitation and groundwater. Limnol Oceanogr. doi: 10.4319/lo.1978.23.4.0798

van Wijnen HJ, Bakker JP (1999) Nitrogen and phosphorus limitation in a coastal barrier salt marsh : The implications for vegetation succession. Br Ecol Soc 87:265–272

Vitousek PM, Aber JD, Howarth RW, et al (1997) Human alteration of the global nitrogen cycle. Ecol Soc Am 7:737–750

Waring RH, Landsberg JJ, Williams M (1998) Net primary production of forest: a constant fraction of gross primary production? Tree Physiol 18:129–134. doi: Doi 10.1039/B400252k

Welschmeyer NA (1994) Flourometric analysis of chlorophyll *a* in the presence of chlorophyll *b* and pheopigments. Limnol Oceanogr 39:1985–1992. doi: 10.1111/j.1540-5931.2009.00571.x

White DS, Howes BL (1994) Long-term ^{15}N retention in the vegetated sediments of a New England salt marsh. Limnol Oceanogr 39:1878–1892

Williams RB, Murdoch MB (1972) Compartmental analysis of the production of *Juncus roemerianus* in a North Carolina salt stable. Coast Estuar Res Fed 13:69–79

Wilson BJ, Mortazavi B, Kiene RP (2015) Spatial and temporal variability in carbon dioxide and methane exchange at three coastal marshes along a salinity gradient in a northern Gulf of Mexico estuary. Biogeochemistry 123:329–347. doi: 10.1007/s10533-015-0085-4

Yin G, Hou L, Liu M, et al (2014) A novel membrane inlet mass spectrometer method to measure $^{15}NH4_4^+$ for isotope-enrichment experiments in aquatic ecosystems. Environ Sci Technol 48:9555–62. doi: 10.1021/es501261s